Journal of Organometallic Chemistry 693 (2008) 3357–3362

Contents lists available at ScienceDirect

Journal of Organometallic Chemistry

journal homepage: www.elsevier.com/locate/jorganchem

Tris-(1,2-*N*,*N*-dimethylaminomethylferrocenyl)stibine and its heterotrimetallic complex

D. Pérez [a], P. Sharma [a,*], N. Rosas [a], A. Cabrera [a], J.L. Arias [b], F. del Rio-Portilla [a], J. Vazquez [a], R. Gutierrez [c], A. Toscano [a]

[a] *Instituto de Química, Universidad Nacional Aútonoma de Mexico, 04510 México D.F., Mexico*
[b] *Facultad de Estudios Superiores Cuautitlán Departamento de Química, UNAM, Cuautitlán Izcalli, Estado de México 54700, Mexico*
[c] *Facultad de Ciencias Químicas, BUAP, Puebla 72001, Mexico*

ARTICLE INFO

Article history:
Received 7 May 2008
Received in revised form 9 August 2008
Accepted 11 August 2008
Available online 15 August 2008

Keywords:
Stibine
Ferrocene
Heterotrimetallic
Platinum complex
Hypervalent antimony

ABSTRACT

New tertiary chloro-bis(1,2-*N*,*N*-dimethylaminomethylferrocenyl)stibine (**1**) and tris-(1,2-*N*,*N*-dimethylaminomethylferrocenyl)stibine ligand (**2**) containing CH_2NMe_2 pendenant arm at the *ortho*-position have been synthesized. Stibine (**2**) reacts with $PtCl_4^{2-}$ and hetero trimetallic *cis*-$PtCl_2L$ (**3**) complex is obtained, where stibine (**2**) acts as a bidentate ligand. All these compounds were characterized by various physicochemical methods and their molecular structures were determined by X-ray diffraction analyses. It is to be noted that tris(1,2-aminomethylferrocenyl)stibine represents the first example of a structurally characterized ferrocenyl pnictogen where three 1,2-disubstituted ferrocenyl groups are attached to the central antimony atom and phosphorus analogue of the stibine is missing in the literature. Stibine (**1**) shows a hypervalent Sb–N interaction while stibine (**2**) does not show this interaction in solid state.

1. Introduction

Recently the chemistry of hypervalent compounds bearing heavier pnictogens (in particular Sb, Bi) has attracted interest [1–6]. Intramolecular interactions between antimony and sp^3-nitrogen atoms have been widely reported [7–13], and 2(Me_2NCH_2)C_6H_4– and 8-(Me_2N)$C_{10}H_6$– moieties have often been applied to stabilize organoantimony molecular complexes, cations, or compounds containing metal–metal bonds [9–13].

Ferrocenylmethyl species (FcN) has been used as ligand over past several years. There are many reports on the silicon, aluminum, and tin substituted FcN derivatives [14–16]. Recently our group has reported the first ferrocenylstibines containing 2-dimethylaminomethyl- and 2-dimethylaminoethyl-side chains and Sb–N hypervalent interactions were observed in their molecular structure [17,18]. In view of the existence of a few reports in the literature on ferrocene bonded antimony and our interest in functionalized triarylstibines ligands, especially those comprising triple substitution in *ortho*-positions [7,19–21] and considering the unique stereoelectronic properties of the ferrocene framework for the synthesis of new ferrocenylstibine dendrimers, here, we wish to report the synthesis and structural characterization of new tertiary chloro-bis(1,2-ferrocenyl)stibine (**2**), tris(1,2-ferrocenyl)stibine ligand (**2**) and heterotrimetallic platinum complex of stibine (**2**).

2. Results and discussion

The yellowish orange crystalline stibine (**1**) and (**2**) were prepared via a salt elimination reaction of 2-lithiated (*N*,*N*-dimethylamino)methylferrocene in 2:1 and 3:1 molar ratio respectively with $SbCl_3$ in ether at −78 °C. Stibine (**2**) forms complex $PtCl_2 \cdot L$ (**3**) after reacting with $[PtCl_4]^{2-}$ in acetone–water as shown in scheme 1.

Stibine (**1**) and (**2**) and platinum complex (**3**) are soluble in polar organic solvents e.g. chloroform, dichloromethane. These compounds are insoluble in water and have little solubility in non polar solvents e.g. hexane, pentane. These two stibine ligands and platinum complex are stable and melt without decomposition.

For all the compounds, the FAB^+ spectra molecular ion peaks were observed along with fragments corresponding to the successive loss of organic entities attached to antimony atom. In the far IR spectra of these compounds, Sb–C vibrations were observed for all the compounds and Pt–Cl vibrations for complex (**3**) have been observed. For all the compounds, the assignment of individual proton signals in the ^1H NMR spectra was based on J_{HH} coupling constant values and was confirmed by COSY and HETCOR experiments. The molecular structures of (**1**), (**2**), and (**3**) have been confirmed by X-ray crystallography as shown in Figs. 1–3. All the

* Corresponding author. Fax: +52 555 6162217.
E-mail address: pankajsh@servidor.unam.mx (P. Sharma).

0022-328X/$ - see front matter © 2008 Elsevier B.V. All rights reserved.
doi:10.1016/j.jorganchem.2008.08.014

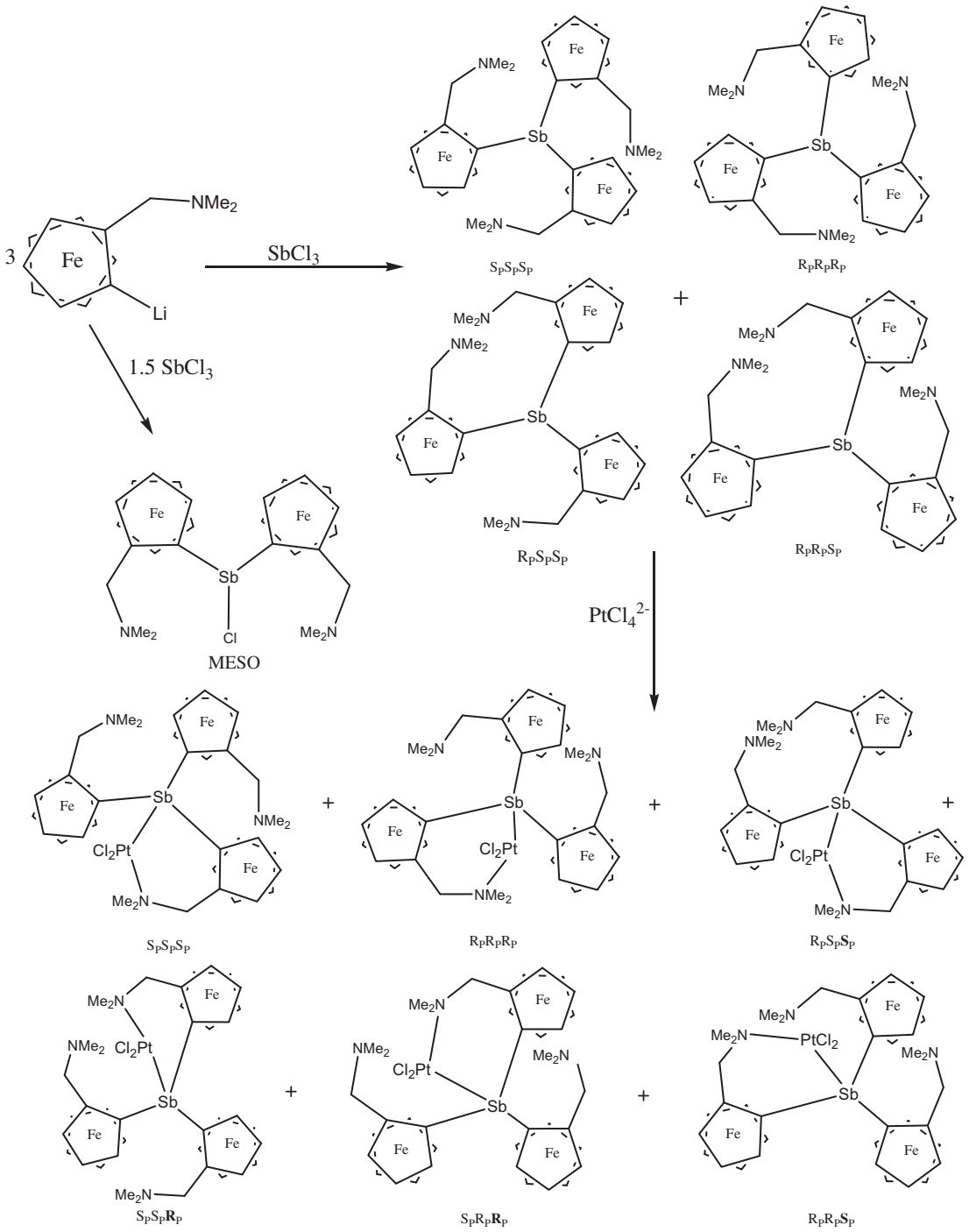

Scheme 1.

three compounds possess planar chirality. The complex (**3**) was crystallized in enantiomerically pure form and corresponds to the diastereoisomer $R_pS_pS_p$ which was confirmed by Flack parameter, while compound (**1**) and (**2**) corresponds to meso (R_p S_p) and $R_pR_pS_p$ ($S_pS_pR_p$) diastereoisomers, respectively.

Though Sb–N interaction was observed in the structural characterizations, evidence for such interaction could not be detected in ^{1}H NMR spectra of stibine (**1**). In ^{1}H NMR spectra of stibine (**1**), in $CDCl_3$ at 25°, both NMe_2 substituents are magnetically equivalent, resulting in only one signal for both methyl groups. However, the methylene protons of the FcN moiety of (**1**) are not magnetically equivalent. This phenomenon has been observed in the ^{1}H NMR spectra of complexes containing both monodentate and bidentate 1,2-disubstituted ferrocenyl ligands [22,23]. It is also a consequence of the asymmetry of the disubstituted Cp ring. The diastereotopic methylene protons give rise to two AB doublets. In the case of (**1**), the doublets are observed at δ 3.68 (d, J_{HH} = 13.76 Hz), δ 3.05 (d, J_{HH} = 13.76 Hz). The ^{1}H NMR data of (1) $(FcN)_2SbCl$ show the presence of only one diastereomer either *rac*- or *meso*- (because of the presence of a C_2-axis in both the diastereomers), in each diastereomer only one set of signals for both FcN groups appears. It was not possible to assign the signal to the appropriate diastereomer. But X-ray crystallographic determination of (**1**), it was found that (**1**) embody the RS-$(FcN)_2SbCl_{(meso)}$.

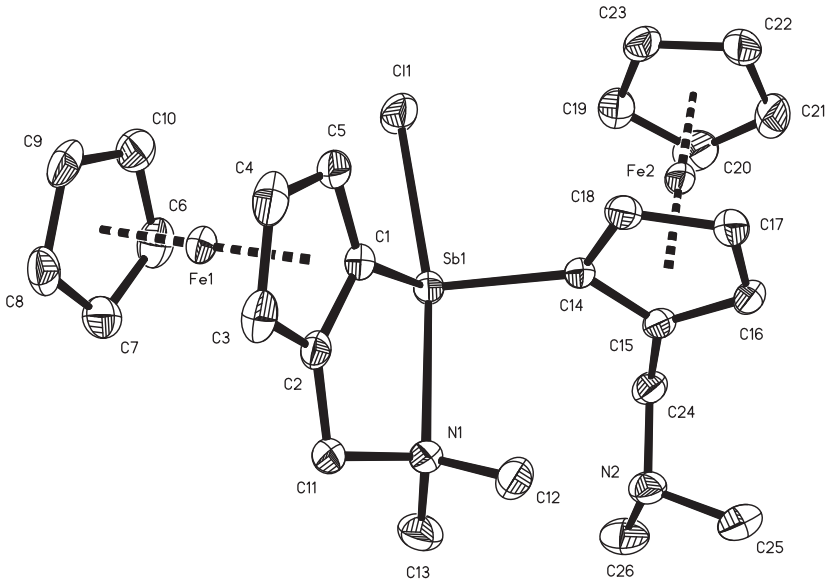

Fig. 1. Molecular structure of chloro-bis(*N*, *N*-1,2-dimethylaminomethylferrocenyl) stibine (**1**).

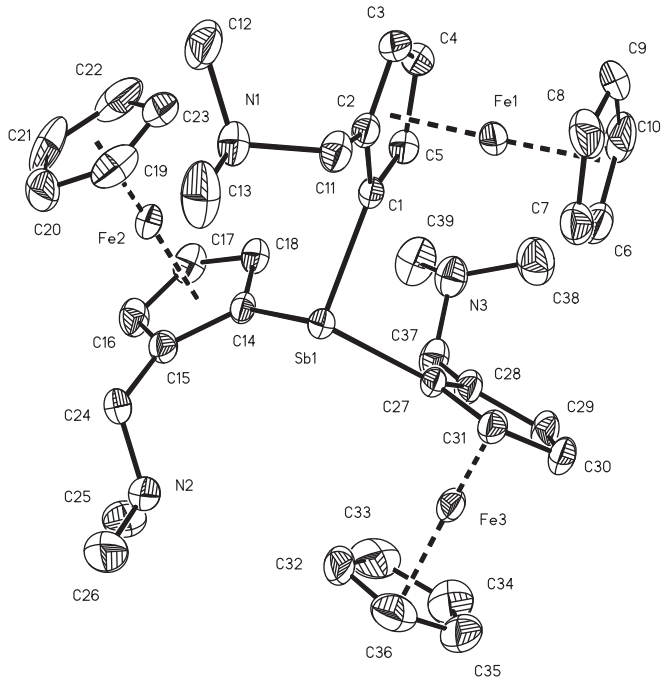

Fig. 2. Molecular structure of tris(*N*,*N*-1,2-dimethylaminomethylferrocenyl)stibine (**2**).

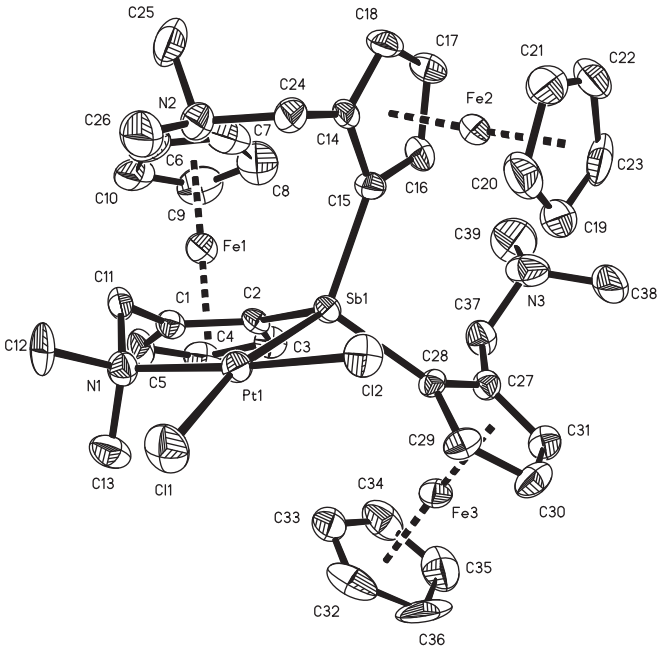

Fig. 3. Molecular structure of *cis*-dichloro [(tris(2-*N*,*N*-dimethylaminomethyl ferrocenyl) stibino-N,Sb)]platinum(II) (**3**).

Considering the crystal structure, one can assume that the ^{1}H NMR spectral assignment is presumably for meso-$(FcN)_2SbCl$ compound. Similarly in the ^{13}C NMR spectra non existence of two set of signals was observed confirming the presence of one diastereomer.

The ^{1}H and ^{13}C NMR spectra of (**2**) and (**3**) clearly demonstrate the magnetic non-equivalence of the proton and carbon nuclei in different FcN ligands. For the complex (**3**), ^{1}H NMR signals appeared at slightly downfield in comparison to the free ligand.

Tris(1,2-*N*,*N*-dimethylaminomethylferrocenyl) stibine ligand (**2**) presents 4 signals for each type of nucleus, ^{1}H and ^{13}C, due to the presence of two pairs of enantiomers. It was possible to distinguish between the $R_pR_pR_p$ or $S_pS_pS_p$ enantiomer pair with $R_pR_pS_p$ or $S_pS_pR_p$ enantiomer pairs. The ligands with C_3 symmetry $R_pR_pR_p$ or $S_pS_pS_p$ are indistinguishable enantiomers within NMR experiments and they show one set of signals (FcN group A type) twice the integrals in comparison with those diastereomers which have lost the C_3 symmetry ($R_pR_pS_p$ or $S_pS_pR_p$ enantiomer, to say FcN group B, C, and D types). Using 2D NMR experiments (COSY, HETCOR, HSQC, HMBC and NOESY), it was possible to assign all signals for the diastereomers present in solution. It could be observed in Fig. 4 that the $R_pR_pS_p$ or $S_pS_pR_p$ enantiomeric pair shall produce three set of signals for each FcN group, as observed in the ^{1}H and ^{13}C NMR experiments. However, it was not possible to differentiate the

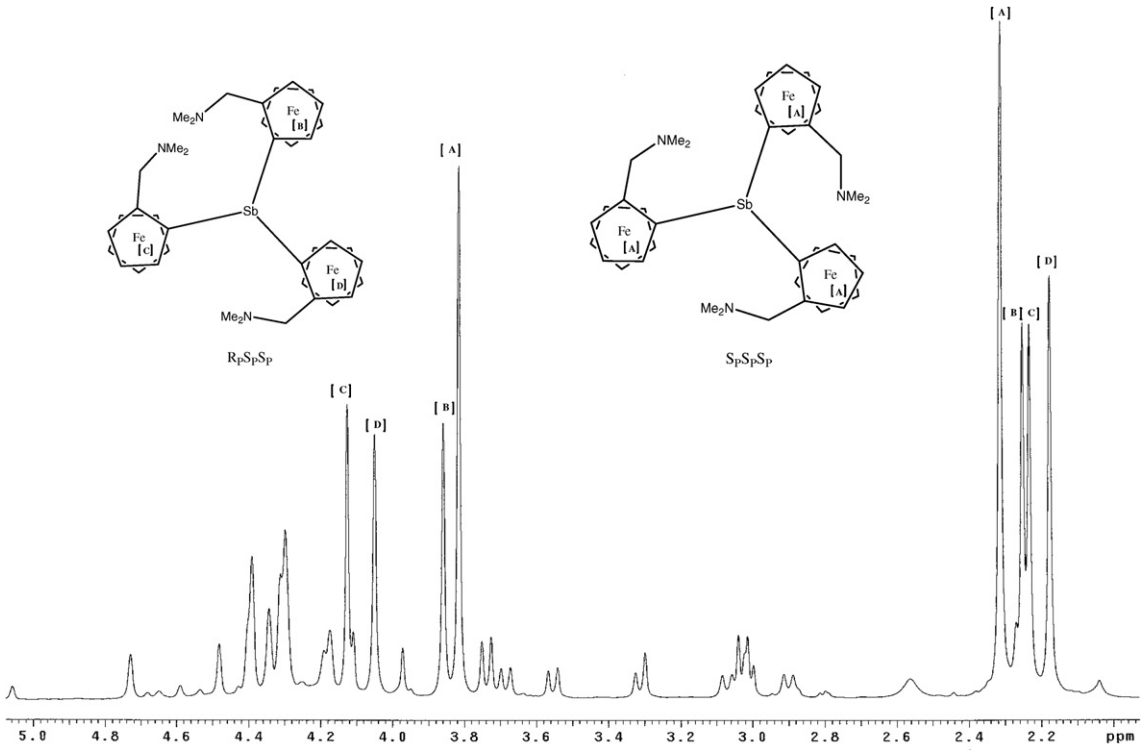

Fig. 4. ^{1}H NMR of stibine (**2**) showing the chemical shifts for two pairs of enantiomers (for complete assignment see Section 3).

FcN groups between types B, C and D. ^{1}H NMR spectra recorded at 40 °C and 60 °C present are not different than room temperature spectrum. Similarly in complex (**3**) there exists three pairs of enantiomers and three set of signals for the complex were observed in the ^{1}H and ^{13}C NMR spectra. It was concluded that the solution of the complex (**3**) shows the presence of six diastereoisomers and a spontaneous resolution occurred upon crystallization and the complex crystallized in enantiomerically pure $R_pS_pS_p$ diastereoisomer.

Crystal data for all structural analyses are given in Table 1. Selected bond lengths and angles for all compounds are listed in Table 2. The average Sb–$C_{(ferrocenyl)}$ bond length found in these ferrocenylstibines is 2.123 Å, which is slightly shorter than that found in the other known tertiary stibines containing Sb-$C_{(aryl)}$ bond, this observation was also reported earlier [17,18]. It is to be noted that tris(1,2-aminomethylferrocenyl)stibine representing the first example of a structurally characterized ferrocenyl pnictogen where three 1,2-disubstituted ferrocenyl rings are attached to the central

Table 1
Crystallographic data for compounds **1–3**

Compounds	**1**	**2**	**3**
Empirical formula	$C_{39}H_{48}Fe_3N_3Sb$	$C_{26}H_{32}ClFe_2N_2Sb$	$C_{39}H_{48}Cl_2Fe_3N_3PtSb^{*}CHCl_3$
Formula weight	848.10	641.44	1233.46
Crystal color and shape	Red prism	Orange plates	Orange prism
Crystal system	Triclinic	Monoclinic	Orthorhombic
Space group	$P\bar{1}$	$C\,2/c$	$P2_12_12_1$
Crystal size (mm)	0.334 × 0.222 × 0.146	0.232 × 0.216 × 0.078	0.168 × 0.136 × 0.112
a (Å)	12.3051(8)	23.725(1)	13.2143(7)
b (Å)	12.4813(8)	12.156(1)	14.1122(7)
c (Å)	14.2224(9)	18.108(1)	23.642(1)
α (°)	67.886(1)	90	90
β (°)	78.059(2)	104.310(1)	90
γ (°)	66.203(1)	90	90
V (Å^3)	1847.7(2)	5060.3(5)	4408.8(4)
Z	2	8	4
D_{calc} (g/cm^3)	1.524	1.684	1.858
μ (mm^{-1})	1.908	2.314	5.065
2θ (°)	1.55–32.48	1.77–25.36	1.68–32.52
Reflections collected	35815	20923	61485
Independent reflections	13068	4631	15946
R_{int}	0.0610	0.0506	0.0769
R_1 [$I > 2\sigma(I)$]	0.0620	0.0277	0.0454
Flack parameter			−0.017(4)
GOF	1.003	0.896	0.981
Max/min $\Delta\rho$ (e Å^{-3})	1.423/−0.700	0.555/−0.458	3.894/−1.491

Table 2
Selected bond length (A°) and selected bond angles (°) for compounds **1**–**3**

Compound **1**		Compound **2**		Compound **3**	
Sb–C1	2.122(3)	Sb–C14	2.138(3)	Sb–C2	2.095(5)
Sb–C14	2.140(3)	Sb–C27	2.140(3)	Sb–C15	2.102(5)
Sb–Cl1	2.538(1)	Sb–C1	2.144(3)	Sb–C28	2.128(5)
Sb–N1	2.553(2)	C14–Sb–C27	103.65(12)	Pt–Sb	2.5162(4)
C1–Sb–C14	98.61(11)	C14–Sb–C1	96.96(12)	Pt–Cl1	2.3450(16)
C1–Sb–Cl1	86.88(8)	C27–Sb–C1	96.93(12)	Pt–Cl2	2.2896(15)
C14–Sb–Cl1	96.77(8)			Pt–N1	2.113(4)
C1–Sb–N1	72.85(9)				
C14–Sb–N1	88.24(9)			C2–Sb–C15	106.8(2)
				C2–Sb–C28	105.9(2)
				C15–Sb–C28	105.6(2)
				C2–Sb–Pt	105.34(14)
				C15–Sb–Pt	120.36(16)
				C28–Sb–Pt	111.95(15)
				N1–Pt–Sb	96.51(12)

antimony atom and phosphorus analogue of this stibine is still missing in the literature.

In compound (**1**) distance between nitrogen atom of one of the NMe_2 group and the central antimony atom is 2.553(2) Å, which is much shorter (68%) than the sum of their Van der Waals radii (3.74 Å). This Sb–N distance is slightly longer than the covalent bond length of 2.11 Å [24]. This result indicates hypervalent bond formation between antimony and nitrogen. This hypervalent Sb–N interaction was not observed in other two compounds (**2**) and (**3**). The structure is very similar to chloro-bis(*N*,*N*-dimethylaminoethylferrocenyl) stibine reported earlier, where Sb–N distance is slightly longer 2.584(5) Å [18]. In this compound, the geometry about antimony atom is distorted pseudo trigonal bipyramid.

In compound (**2**), the geometry around the antimony atom is distorted tetrahedral with one lone pair of electron and the molecule has a pyramidal geometry. The average Sb–C distances fall within the limits found in related organoantimony structures.

The platinum complex crystallizes with one molecule of chloroform as a solvent of crystallization. A very few structures of platinum stibine complexes are reported in literature. In this heterotrimetallic complex, the stibine ligand (**2**) acts as a bidentate chelating Sb, N-type ligand. Platinum is in square planar geometry and the Pt–Sb bond length (2.516 Å) found in compound is similar to the Pt–Sb bond length observed in reported *cis*-[$PtCl_2(SbPh_3)_2$] complex [2.502(1) Å] [25] and *cis*-dichloro[(tris(2-*N*,*N*-dimethylaminomethylferrocenyl)phenylstibino-N,Sb)]platinum(II) (2.494 Å) [7]. The Pt–Cl bond *trans* to antimony is 2.345 Å and is shorter than the Pt–Cl bond length reported in *cis*-[$PtCl_2Sb(C_6H_4CH_2NMe_2)_3$] (2.360 Å), where the ligand behaves in bidentate fashion. The geometry around antimony is distorted tetrahedral. This is the third structural determination of a Pt–stibine complex containing a Pt–Cl bond *trans* to stibine ligand.

3. Experimental

All the solvents were distilled immediately prior to use. All the reactions were performed under an atmosphere of oxygen-free, dry nitrogen. Melting points were obtained on a MEL-TEMP II Fisher and are uncorrected. EI and FAB^+ mass spectra were recorded on a JEOL SX102 double-focusing mass spectrometer with reverse geometry using a 6-kV Xenon beam (10 am); nitrobenzyl alcohol was used as matrix for recording the mass spectra. IR spectra were recorded on a Nicolet-Magna 750 FT-IR spectrometer as nujol mulls. ^1H and ^{13}C NMR spectra were recorded in $CDCl_3$ on a JEOL ECLIPSE 300 (^1H: 300.5311 MHz; ^{13}C: 75.5757 MHz) and on a VARIAN UNITY INOVA 500 (^1H: 499.98 MHz; ^{13}C: 125.73 MHz) spectrometers. Chemical shift were referenced with internal TMS. Signals were assigned using 1D ^1H and ^{13}C, and 2D COSY, HETCOR, HSQC, HMBC and NOESY (0.6 s mixing time) experiments.

3.1. X-ray crystallography

The X-ray intensity data were measured at 293 K on a Bruker SMART APEX CCD-based X-ray diffractometer using a monochromatized Mo Kα radiation (kα 0.71073 Å). The detector was placed at a distance of 4.837 cm from the crystals in all cases. Analysis of the data showed in all cases negligible decays during data collections. An analytical face indexed absorption correction was applied. Crystal structures were refined by full-matrix least squares. SMART software (data collection and data reduction) and SHELXTL were used for solution and refinement of the structures.

3.2. Syntheses

3.2.1. Synthesis of chloro-bis(N,N-dimethylaminomethylferrocenyl)-stibine (*1*)

A solution of antimony trichloride (1.36 g, 6 mmol) in ether (10 ml), α(*N*,*N*-dimethylamino)methylferrocenyl lithium (2.95 g, 11.8 mmol) {synthesized *in situ* according to reported method [14]}, was added dropwise under a nitrogen atmosphere at −20 °C with continuous stirring. The mixture was further stirred for 24 h at room temperature and then reaction was quenched with ice. After extraction with dichloromethane (3 × 10 ml) and drying over sodium sulfate, solvent was removed under vacuum. The compound was dried and recrystallized from chloroform and after concentration gives the orange product. Yield 59%; m.p. 135–137 °C; IR (ν cm^{-1}): 492 (Sb–C), 3094 (C–H aromatic). FAB^+ *m/z*: 641 (4%) $[M]^+$, 605 (100%) $[M–Cl]^+$, 517 (12%) $[M–Cl–2NMe_2]$, 363 (13%) $[M–FcCH_2\ NMe_2Sb]^+$, 242 (23%) $[FcCH_2\ NMe_2]^+$; ^1H NMR ($CDCl_3$, δ in ppm): 2.17 (s, 12H, N*Me*$_2$), 3.05 (d, J_{HH} = 13.76 Hz, 2H, CH_2), 3.68 (d, J_{HH} = 13.76 Hz, 2H, CH_2), 4.23 (s, 10H, C*H*, C_5H_5), 4.21–4.26 (m, 6H, C*H*, C_5H_3); ^{13}C NMR ($CDCl_3$, δ in ppm): 46.16 (N*Me*$_2$), 60.00 (*C*H_2), 69.34 (*C*H, C_5H_3), 69.65 (*C*H, C_5H_3), 69.75 (*C*H, C_5H_5), 73.25 (*C*H, C_5H_3), 86.93 (*C*–Sb), 90.86 (*C*–CH_2).

3.2.2. Synthesis of tris(N,N-dimethylaminomethylferrocenyl)stibine (*2*)

A solution of antimony trichloride (0.75 g, 3.3 mmol) in ether (10 ml), α(*N*,*N*-dimethylamino)ethylferrocenyllitium (2.49 g, 10 mmol) {synthesized *in situ* according to reported method [14]}, was added dropwise under a nitrogen atmosphere at −20 °C with continuous stirring. The mixture was further stirred for 24 h at room temperature and then reaction was quenched with ice. After extraction with dichloromethane (3 × 10 ml) and drying over sodium sulfate, solvent was removed under vacuum. The compound was dried and recrystallized from chloroform and after concentration gives the orange product. Yield 59%; m.p. 128–130 °C; IR (ν cm^{-1}): 492 (Sb–C), 3094 (C–H aromatic). EI *m/z*: 847 (26%) $[M]^+$, 803 (35%) $[M–NMe_2]^+$, 715 (8%) $[M–3NMe_2]^+$, 605 (57%) $[M–FcCH_2\ NMe_2]^+$, 363 (13%) $[SbFcCH_2NMe_2]^+$, 242 (97%) $[FcCH_2NMe_2]^+$; ^1H NMR ($CDCl_3$, δ in ppm): $R_pR_pR_p$ and $S_pS_pS_p$: 2.32 (s, 6H, N*Me*$_2$), 3.04 (d, 12.5 Hz, 1H, CH_2), 3.75 (d, 12.5 Hz, 1H, CH_2), 3.82 (s, 5H, C*H*, C_5H_5), 4.31 (s, 2H, C_5H_3), 4.40 (s, 1H, C_5H_3); ^{13}C NMR ($CDCl_3$, δ in ppm): 45.69 (N*Me*2), 60.55 (*C*H2), 69.56 (*C*H, C_5H_5), 69.60 (*C*H, C_5H_3), 71.14 (*C*H, C_5H_3), 74.67 (*C*H, C_5H_3), 75.85 (C–Sb), 89.97 (*C*–CH_2); $R_pR_pS_p$, type B: ^1H NMR ($CDCl_3$, δ in ppm): 2.26 (s, 6H, N*Me*$_2$), 3.02 (d, 12.3 Hz, 1H, CH_2), 3.69 (d, 12.3 Hz, 1H, CH_2), 3.87 (s, 5H, C*H*, C_5H_5), 4.35 (m, 1H, C_5H_3), 4.42 (m, 1H, C_5H_3), 4.74 (m, 1H, C_5H_3); ^{13}C NMR ($CDCl_3$, δ in ppm): 45.87 (N*Me*2), 60.54 (*C*H_2), 69.60 (*C*H, C_5H_5), 69.79 (*C*H, C_5H_3), 71.94 (*C*H, C_5H_3), 76.24 (*C*H, C_5H_3), 75.55 (C–Sb), 89.97 (*C*–CH_2); type C: ^1H NMR ($CDCl_3$, δ in ppm): 2.24 (s, 6H, N*Me*$_2$), 3.08

(d, 13.3 Hz, 1H, CH_2), 3.56 (d, 13.3 Hz, 1H, CH_2), 4.14 (s, 5 H, C*H*, C_5H_5), 4.18 (s, 1H, C*H*, C_5H_3), 4.32 (m, 1H, C*H*, C_5H_3), 4.35 (m, 1H, C*H*, C_5H_3); ^{13}C NMR ($CDCl_3$, δ in ppm): 45.46 (N*Me*2), 59.62 (*C*H_2), 69.34 (*C*H, C_5H_5), 69.6 (*C*H, C_5H_3), 75.72 (*C*H, C_5H_3), 71.30 (*C*H, C_5H_3), 72.83 (*C*–Sb), 89.95 (*C*–CH_2); type D: ^{1}H NMR ($CDCl_3$, δ in ppm): 2.19 (s, 6H, N*Me*$_2$), 2.91 (d, 12.8 Hz, 1H, CH_2), 3.32 (d, 12.8 Hz, 1H, CH_2), 4.06 (s, 5H, C*H*, C_5H_5), 4.31 (s, 1H, C*H*, C_5H_3), 4.40 (m, 1H, C*H*, C_5H_3), 4.49 (m, 1H, C*H*, C_5H_3); ^{13}C NMR ($CDCl_3$, δ in ppm): 45.64 (N*Me*2), 59.62 (*C*H_2), 69.28 (*C*H, C_5H_5), 69.6 (*C*H, C_5H_3), 72.82 (*C*H, C_5H_3), 76.87 (*C*H, C_5H_3), 71.57 (*C*–Sb), 89.90 (*C*–CH_2).

3.2.3. cis-Dichloro [(tris(2-N,N-dimethylaminomethylferrocenyl)-stibino-N,Sb)]platinum(II) (**3**)

To a solution of (**2**) (0.19 mmol) in acetone (20 ml) was added K_2PtCl_4 in water. The mixture was stirred for 12 h. The resultant mixture was filtered to remove any undissolved material and filtrate was concentrated to obtain a yellow powder, which was recrystallized from chloroform–hexane mixture (80:20). Yield: 40%; m.p. 128–130 °C; IR (ν cm^{-1}): 490 (Sb–C), 3090 (C–H aromatic), 317 and 325 (Pt–Cl); FAB$^+$ *m/z*: 1113 (9%) [M]$^+$, 1069 (4%) [M– NMe_2]$^+$, 1043 (8%) [M–2Cl]$^+$, 834 (2%) [M–Cl_2FcCH_2]$^+$, 800 (8%) [M–$Cl_2FcCH_2NMe_2$], 605 (8%) [M–$PtCl_2FcCH_2NMe_2$]$^+$, 363 (9%) [$SbFcCH_2NMe_2$]$^+$, 242 (100%) [$FcCH_2NMe_2$]$^+$; ^{1}H NMR ($CDCl_3$, δ in ppm): 2.94 (d, 1H, CH_2), 3.01 (d, 1H, CH_2), 3.15 (d, 1H, CH_2), 3.34 (d, 1H, CH_2), 3.53 (d, 1H, CH_2), 3.72(d, 1H, CH_2), 2.19 (s, 6H, NMe_2), 2.28 (s, 6H, NMe_2), 2.29 (s, 6H, NMe_2), 3.82 (s, 5H, C*H*, C_5H_5), 4.15 (s, 5H, C*H*, C_5H_5), 4.37 (m, 5H, C*H*, C_5H_5), 3.84 (m, 3H, C*H*, C_5H_3), 4.08 (m, 3H, C*H*, C_5H_3), 4.22 (m, 3H, C*H*, C_5H_3); ^{13}C NMR ($CDCl_3$, δ in ppm): 45.49 (NMe_2), 45.78 (NMe_2), 45.84 (NMe_2), 59.63 (CH_2), 60.50 (CH_2), 60.55 (CH_2), 69.29 (C*H*, C_5H_5), 69.45 (C*H*, C_5H_5), 69.54 (C*H*, C_5H_5), 70.48 (C*H*, C_5H_3), 71.16 (C*H*, C_5H_3), 71.34 (C*H*, C_5H_3), 71.94 (C*H*, C_5H_3), 72.83 (C*H*, C_5H_3), 73.26 (C*H*, C_5H_3), 73.76 (C*H*, C_5H_3), 74.03 (C*H*, C_5H_3), 74.6 (C*H*, C_5H_3), 79.24 (*C*–Sb), 79.86 (*C*–Sb), 79.95 (*C*–Sb) .

4. Supplementary material

CCDC 681012 and 681014 contain the supplementary crystallographic data for compounds **1**–**3**. These data can be obtained free of charge from The Cambridge Crystallographic Data Centre via www.ccdc.cam.ac.uk/data_request/cif.

Acknowledgements

Authors are thankful to DGAPA(IN205507) for financing the work. We are also thankful to Ing. Luis Velasco Ibarra and Dr. Javier Perez Flores for their assistance in mass spectral studies.

References

[1] T. Murafuji, T. Mutoh, K. Satoh, K. Tsunenari, N. Azuma, H. Suzuki, Organometallics 14 (1995) 3848.
[2] M. Weinman, A. Gehrig, B. Schiemenz, G. Huttner, B. Nuber, G. Reiwald, H. Lang, J. Organomet. Chem. 563 (1998) 61.
[3] Y. Takaguchi, A. Hosowaka, S. Yamada, J. Motoyoshishya, H. Aoyama, J. Chem. Soc. Perk. Trans. I (1998) 3147.
[4] D.A. Atwood, A.H. Cowley, J. Ruiz, Inorg. Chim. Acta 198–200 (1992) 271.
[5] H. Suzuki, T. Murafuji, Y. Matano, N. Azuma, J. Chem. Soc., Perkin Trans. 1 (1993) 2969.
[6] P. Sharma, D. Pérez, N. Rosas, A. Cabrera, A. Toscano, J. Organomet. Chem. 691 (2006) 579.
[7] P. Sharma, D.A. Castillo, N. Rosas, A. Cabrera, E. Gomez, A. Toscano, F. Lara, S. Hernandez, G. Espinosa, J. Organomet. Chem. 689 (2004) 2593.
[8] C.J. Carmalt, A.H. Cowley, R.D. Culp, R.A. Jones, S. Kamepalli, N.C. Norman, Inorg. Chem. 36 (1997) 2770.
[9] T. Tokunaga, H. Seki, S. Yasuike, M. Ikoma, J. Kurita, K. Yamaguchi, Tetrahedron 56 (2000) 8833.
[10] T. Tokunaga, H. Seki, S. Yasuike, M. Ikoma, J. Kurita, K. Yamaguchi, Tetrahedron Lett. 41 (2000) 1031.
[11] H.J. Breunig, I. Ghesner, M.E. Ghesner, E. Lork, Inorg. Chem. 42 (2003) 1751.
[12] L.M. Opris, A. Silvestru, C. Silvestru, H.J. Breunig, E. Lork, J. Chem. Soc. Dalton Trans. (2003) 4367.
[13] S. Kamepalli, C.J. Karmalt, R.D. Culp, A.H. Cowley, R.A. Jones, N.C. Norman, Inorg. Chem. 35 (1996) 6179.
[14] K. Jacob, N. Siedel, F. Voigt, A. Fischer, C. Pietzsch, J. Holecek, A. Lycka, M. Fontani, E. Grigiotti, P. Zanello, J. Prackt. Chem. 342 (2000) 574.
[15] F. Voigt, K. Jacob, N. Seidel, C. Pietzsch, P. Zanello, J. Prakt. Chem. 342 (2000) 666.
[16] K. Jacob, Z. Anorg. Allg. Chem. 630 (2004) 197.
[17] P. Sharma, J.G. Lopez, C. Ortega, N. Rosas, A. Cabrera, C. Alvarez, A. Toscano, E. Reyes, Inorg. Chem. Commun. 9 (2006) 85.
[18] J. Vazquez, P. Sharma, A. Cabrera, A. Toscano, S. Hernández, J. Perez, R. Gutierrez, J. Organomet. Chem. 692 (2007) 3486.
[19] R.M. Gomez, P. Sharma, J.L. Arias, J.F. Perez, L. Velasco, A. Cabrera, J. Mol. Catal. (A) 170 (2001) 271.
[20] A. Cabrera, P. Sharma, J.L. Arias, J.F. Perez, L. Velasco, R.M. Gomez, J. Mol. Catal. (A) 212 (2004) 19.
[21] P. Sharma, A. Cabrera, R. Lagadec, R. Manzo, J.L. Arias, M. Sharma, Main Group Met. Chem. 22 (1999) 95.
[22] J. Azizizan, R.M.G. Roberts, J. Silver, J. Organomet. Chem. 303 (1986) 397.
[23] R.V. Honeychuck, M.O. Okoroafor, L.-H. Shen, C.H. Brubaker, Organometallics 5 (1986) 482.
[24] J. Emsley, The Elements, third ed., Clarendon, Oxford, 1998.
[25] O.F. Wendt, A. Scodinu, L.I. Elding, Inorg. Chim. Acta 277 (1998) 237.